Efficient, Structured Controller Synthesis for Linear Parameter-Varying Systems

Emily Burgin*, Harald Pfifer**

***Abstract*—A structured output-feedback controller synthesis in linear fractional transformation (LFT) formulation is derived. It is presented as a novel approach to the control of linear parameter-varying systems. The LFT formulation leads to a controller synthesis with no approximation steps and it scales better than a gridded formulation when increasing the number of scheduling parameters. The proposed approach has better computational efficiency than a traditional output-feedback controller synthesis, as it solves two small semi-definite programs (SDP) in a two step synthesis, rather than one large SDP posed by the traditional approach. This two-step synthesis also results in the controller's fixed structure. The design process uses a recently proposed weighting scheme to impose unambiguous, tractable and physically interpretable closed-loop performance requirements; suitable for use on many aerospace applications. An exemplary spacecraft control problem demonstrates the computational superiority of the novel approach over standard output-feedback synthesis when using different scheduling parameters. There is also minimal loss in performance in the structured controller compared to the output-feedback controller.**

***Index Terms*—Robust control, aerospace control, linear matrix inequalities**

I. Introduction

MANY aerospace problems are highly parameter-dependent. For example, an aircraft's dynamics vary significantly over altitude and velocity [1], or a spacecraft's dynamics can vary with the orientation of a movable solar array [2]. When designing a control scheme for such applications, linear parameter-varying (LPV) controller design (recent applications in, e.g., [3]–[5]) provides an elegant alternative to traditional gain scheduling; it explicitly respects the parameter dependence of the system in the synthesis. Moreover, it is a logical step following the popular $\mathcal{H}_\infty$ framework as it inherits many of the same performance quantifications and thus design principles. The performance of a controlled LPV system is often specified in terms of the induced $\mathcal{L}_2$-norm of the closed-loop, so, well documented and validated design schemes are easily applicable (e.g. mixed-sensitivity). This means that creating and tuning a good controller design scheme in the LPV framework is intuitive and comprehensible. For a thorough summary of LPV techniques over the years, the reader is referred to [6].

This paper was produced at the Chair of Flight Mechanics and Control, Technische Universität Dresden. Correspondence: *emily.burgin@tu-dresden.de, **harald.pfifer@tu-dresden.de

This work was supported by the ESA OSIP co-funded research program under the contract 4000140113/22/NL/GLC/my, titled *AI-Enhanced Real-Time Identification and LFT-Based Control for Space Systems*

There are several special classes of LPV systems that are categorised based on how the state matrices depend on the scheduling parameters. In case of an arbitrary dependence, the LPV controller synthesis problem results in an infinite collection of parameter-dependent linear matrix inequalities (LMIs) [7]. The computational solution of such parameter-dependent LMIs requires some finite-dimensional approximation on a gridded domain. This approach does not scale well with the number of scheduling parameters. To remedy this, the LPV system can be written in a linear fractional representation, provided that the dependence of the state-space matrices on the scheduling parameter can be closely approximated by a rational function. In this case, finite dimensional semidefinite programs (SDPs) can be formulated to synthesise a controller [8], [9]. While generally the linear fractional transformation (LFT) based framework scales more gracefully with the number of scheduling parameters, its computational complexity still prevents wide-spread industrial application in aerospace [10]. It is estimated that up to 38% of a spacecraft control design project's time-budget is spent on the design and tuning phases [11], with the remaining costs going to simulator development, analysis, verification, validation and so on. It is well understood that, in practice, controller design is an iterative process, which involves re-tuning and re-synthesising a controller several times. Therefore, the efficiency of the design process is significantly impacted by the computational efficiency of the synthesis algorithms.

Proposed in this paper is a novel LPV synthesis approach based on the LFT framework that significantly reduces the computational burden of the synthesis. It does this by separating the synthesis SDP into two smaller SDPs, namely a filter synthesis and a state-feedback controller synthesis. Unlike prior work [12], the proposed approach offers guaranteed closed-loop performance bounds. Moreover, it uses a mixed-sensitivity weighting scheme [13] with a minimal amount of physically interpretable weights that are derived directly from the robustness and performance requirements of the controller. Finally, the resulting LPV controller has a fixed structure. This can be further exploited to include, for example, anti-windup compensation. The proposed method is an extension of the author's previous work for gridded LPV systems [14] by application of the full block S-Procedure [15]. It also extends the results therein [14] by the inclusion of dynamic weights in the derivation, as these are typically required to formulate a practical LPV control problem. Related to the main result presented here is also the work of Prempain [16], [17] which proposes a structured control design using Glover and McFarlane's loopshaping procedure [18]. This was

extended by Pereira and de Oliveira [19] to discrete-time applications.

In summary, this paper contributes a novel LFT-LPV synthesis framework which can be used to efficiently synthesise an LPV controller that has a fixed structure. The derivation of the two-step synthesis approach is presented in Section III. Included within this section (in III-B and III-C), the two synthesis SDPs are derived. Finally, the approach is demonstrated in Section IV on the design of a spacecraft attitude controller in a slewing scenario.

II. Preliminaries

LPV systems are a type of system whose dynamics depend continuously on a measurable, time-varying parameter vector $\rho : \mathbb{R} \to \mathcal{P}$, where $\mathcal{P} \in \mathbb{R}^n$ is a compact subset of allowable parameters. Additionally, the parameter variation rate $\dot{\rho}$ is assumed to lie within a hyper-rectangle $\dot{\mathcal{P}}$ defined by $\dot{\mathcal{P}} = \{\dot{\rho}(t) \in \mathbb{R}^n | \, |\dot{\rho}_i(t)| \leq \nu_i, i = 1, \ldots, n\}$. Hence, the set of all admissible trajectories is $\mathcal{T} = \{\rho : \mathbb{R} \to \mathcal{P} | \, \rho \in \mathcal{C}^1, \rho(t) \in \mathcal{P}$ and $\dot{\rho}(t) \in \dot{\mathcal{P}} \; \forall t \geq 0\}$. The parameter ρ is referred to as the scheduling parameter of the dynamic system.

A state-space representation of an n_x^{th}-order LPV system P is defined as

$$P : \left[\begin{array}{c} \dot{x}(t) \\ \hline y(t) \end{array}\right] = \left[\begin{array}{c|c} A(\rho(t)) & B(\rho(t)) \\ \hline C(\rho(t)) & D(\rho(t)) \end{array}\right] \left[\begin{array}{c} x(t) \\ \hline u(t) \end{array}\right], \quad (1)$$

where $x(t) \in \mathbb{R}^{n_x}$ is the state vector, $u(t) \in \mathbb{R}^{n_u}$ the input vector, and $y(t) \in \mathbb{R}^{n_y}$ the output vector. *In this paper the dependence on t is later omitted to shorten the notation*. Given that the system dynamics are a continuous function of the scheduling parameter, it can be stated that $A : \mathcal{P} \to \mathbb{R}^{n_x \times n_x}$, $B : \mathcal{P} \to \mathbb{R}^{n_x \times n_u}$, $C : \mathcal{P} \to \mathbb{R}^{n_y \times n_x}$, and $D : \mathcal{P} \to \mathbb{R}^{n_y \times n_u}$.

Any rational matrix valued function can be formulated into an LFT, so, LPV systems that can be described (or reasonably approximated) by rational functions can be represented in the LFT framework. For example, the state matrix A is cast into an LFT with a partitioned constant matrix $\bar{A}$ and parameter-dependent matrix $\Delta \in \mathbb{R}^{m_1 \times n_1}$, where

$$\bar{A} = \left[\begin{array}{c|c} \bar{A}_{11} & \bar{A}_{12} \\ \hline \bar{A}_{21} & \bar{A}_{22} \end{array}\right] \in \mathbb{R}^{(n_1+n_2)\times(m_1+m_2)}. \quad (2)$$

The upper LFT $F_u(\bar{A}, \Delta(\rho(t)))$ is defined as

$$F_u(\bar{A}, \Delta(\rho(t))) = \bar{A}_{22} + \bar{A}_{21}\Delta(\rho(t))(I - \bar{A}_{11}\Delta(\rho(t)))^{-1}\bar{A}_{12}, \quad (3)$$

where $\Delta(\rho(t))$ takes a diagonal form

$$\Delta(\rho(t)) = \begin{bmatrix} \rho_1(t) I_{s_1} & & \\ & \ddots & \\ & & \rho_{n\delta}(t) I_{s_{n\delta}} \end{bmatrix}. \quad (4)$$

Moreover, the performance of an LPV system can be specified in terms of its induced $\mathcal{L}_2$-norm

$$\|P\| = \sup_{u \in \mathcal{L}_2 \setminus \{0\}, \, \rho \in \mathcal{T}, \, x(0)=0} \frac{\|y\|_2}{\|u\|_2}. \quad (5)$$

A generalisation of the Bounded Real Lemma (BRL) [7] provides a sufficient condition to upper bound $\|P\|$, as stated by the following theorem.

Theorem 1. P is exponentially stable and $\|P\| \leq \gamma$ if there exists a continuously differentiable symmetric matrix function $X(p) : \mathcal{P} \to \mathbb{R}^{n_x \times n_x}$ such that $X(p) \geq 0$ and

$$\begin{bmatrix} X(p)A(p) + A^\top(p)X(p) + \partial X(p,q) & X(p)B(p) \\ B^\top(p)X(p) & -I \end{bmatrix} + \frac{1}{\gamma^2}\begin{bmatrix} C^\top(p) \\ D^\top(p) \end{bmatrix}\begin{bmatrix} C(p) & D(p) \end{bmatrix} \leq 0 \quad (6)$$

hold for all $p \in \mathcal{P}$ and $q \in \dot{\mathcal{P}}$, where $\partial X(p,q) = \sum_{i=1}^{n} \frac{\partial X}{\partial \rho_i}(p) q_i$.

Theorem 1 forms the basis for the induced $\mathcal{L}_2$-norm controller synthesis (see the work of Wu [7]). Consider an open-loop LPV system P_{aug} that is augmented from an open-loop plant P (1) to have additional performance inputs w and outputs z. The objective is to synthesise an output-feedback controller K_{OF}

$$K_{OF} : \left[\begin{array}{c} \dot{x}_K \\ \hline u \end{array}\right] = \left[\begin{array}{c|c} A_K(\rho) & B_K(\rho) \\ \hline C_K(\rho) & D_K(\rho) \end{array}\right] \left[\begin{array}{c} x_K \\ \hline y \end{array}\right], \quad (7)$$

such that the induced $\mathcal{L}_2$-gain of the closed-loop interconnection of P_{aug} and K_{OF}, denoted by the lower fractional transformation $F_l(P_{aug}, K_{OF})$, is minimised $\min_{K_{OF}} \|F_l(P_{aug}, K_{OF})\|$. The purpose of the augmentation is such that when the induced $\mathcal{L}_2$-gain of the closed-loop interconnection is minimised, specified closed-loop behaviour is imposed on the resulting controller. This optimisation problem can be solved via parametrised LMI conditions. The derivation and proof of this is provided in the thesis of Wu [20]. For an LPV system, these LMI conditions are infinite dimensional due to the dependency on ρ. Therefore they can be solved by approximating the system along a grid. Alternatively, if the LPV system is formulated as an LFT, the full block S-Procedure (see next section) can be applied in such a way that the parameter-dependent constraints are satisfied. This leaves a set of LMI conditions that are not parameter-dependent, and thus the optimisation problem is solvable.

A. Full Block S-Procedure

A general approach for transforming a linear parametric matrix inequality from a quadratic form $X(p) = G^\top(p)X_0G(p) < 0$ to a linear form using block multipliers was first proposed by Scherer et al. [15]. The process is known as the full block S-Procedure and it can be applied in such a way that all parameter-dependent constraints are automatically satisfied. In order for this to work, first the parameter dependency must be rational and the quadratic inequality must be expressed with outer factors $G(p)$ as LFTs such that

$$X(p) = G^\top(p)X_0G(p), \text{ and } G(p) = F_u(G_0, \Delta(p)), \quad (8)$$

where the matrix part of the upper LFT G_0 can be partitioned as in (2) into G_{11}, G_{12}, G_{21} and G_{22}. The following theorem states the full block S-Procedure. *For clarity throughout this paper, off-diagonal blocks of block-diagonal matrices are omitted from notation.*

Theorem 2. (Full Block S-Procedure [21]). The quadratic matrix inequality, $X(p) < 0$, that satisfies (8) and $X_0 \in \mathbb{S}^{n_2 \times n_2}$, holds for all $p \in \mathcal{P}$ if and only if there exists a symmetric full block multiplier $\Pi \in \mathbb{S}^{(n_1+m_1)\times(n_1+m_1)}$ such that

$$\left[\begin{array}{c|c} G_{11} & G_{12} \\ I & 0 \\ \hline G_{21} & G_{22} \end{array}\right]^\top \left[\begin{array}{c|c} \Pi & \\ \hline & X_0 \end{array}\right] \left[\begin{array}{c|c} G_{11} & G_{12} \\ I & 0 \\ \hline G_{21} & G_{22} \end{array}\right] < 0 \quad (9)$$

and

$$\left[\begin{array}{c} I \\ \Delta(p) \end{array}\right]^\top \Pi \left[\begin{array}{c} I \\ \Delta(p) \end{array}\right] \geq 0 \ \forall \Delta \in \Delta_s, \quad (10)$$

where Δ_s is a compact set.

Proof. The proof is provided in the work of Wu et al. [21].

Inequality (10) is infinite dimensional, thus the form of multiplier Π must be restricted in order for the problem to be computationally solvable. Three different multipliers are considered in this work, namely a diagonal multiplier, a full-block multiplier and a parameter-dependent multiplier. These three are ordered in decreasing conservatism introduced to the optimisation. This reduced conservatism does, however, result in increased computational burden.

Block-diagonal multiplier

Firstly, the block-diagonal multiplier restricts Π to a symmetric form, so the set of multipliers is defined as

$$\Pi_d := \{\Pi = \left[\begin{array}{cc} -\tilde{R} & \tilde{S} \\ \tilde{S}^\top & \tilde{R} \end{array}\right]\}, \quad (11)$$

where $\tilde{R} = \text{diag}(\tilde{R}_1, ..., \tilde{R}_{n_\delta})$, $\tilde{R} \leq 0$, $\tilde{S} = \text{diag}(\tilde{S}_1, ..., \tilde{S}_{n_\delta})$, $\tilde{S}_i = -\tilde{S}_i^\top$ and both are of appropriate dimensions. Then condition (10) is automatically fulfilled. This works under the assumption that the parameter dependent block $\Delta(p)$ takes the form in (4) with $p \in \Pi := \{p \in \mathbb{R}^{n_\delta} \mid \|p_i\| \leq 1, i = 1, \ldots, n_\delta\}$, which can always be satisfied through normalisation.

Consider the expansion of (10) with the multiplier structure (11) for one parameter p_i

$$\tilde{S}_i p_i + p_i^\top \tilde{S}_i^\top - \tilde{R}_i + p_i^\top \tilde{R}_i p_i \quad (12a)$$

$$= p_i \underbrace{(\tilde{S}_i + \tilde{S}_i^\top)}_{=0} + \underbrace{(p_i^2 - 1)}_{\leq 0} \underbrace{\tilde{R}_i}_{\leq 0} \geq 0. \quad (12b)$$

Given the block-diagonal structure of the multiplier, expanding the left hand side of (10) for all elements results in a block-diagonal matrix where the ith block corresponds to the expansion (12). Given that (12) holds $\forall i$, the block-diagonal matrix must also be positive semidefinite and (10) is satisfied.

Full-block multiplier

The block-diagonal multiplier is a subset of the full-block multiplier which assumes that the set Δ_s is a convex hull of a finite set $\bar{\Delta} = \{\Delta_1, ..., \Delta_n\}$. The set of multipliers is then

$$\Pi_f := \{\Pi = \left[\begin{array}{cc} \tilde{Q} & \tilde{S} \\ \tilde{S}^\top & \tilde{R} \end{array}\right] | \tilde{R} \leq 0\}. \quad (13)$$

Given that the south-east block of $\Pi \in \Pi_f$ is negative semidefinite, the mapping

$$\Delta \leftrightarrow \left[\begin{array}{c} I \\ \Delta \end{array}\right]^\top \Pi \left[\begin{array}{c} I \\ \Delta \end{array}\right] \quad (14)$$

is concave. Hence positivity at $\Delta \in \bar{\Delta}$ implies positivity for all $\Delta \in \Delta_s$. Thus, it is sufficient to evaluate (10) at the vertices of $\bar{\Delta}$, which implies that (10) holds $\forall \Delta \in \Delta_s$. This results in an additional n LMI conditions. For further proof the reader is referred to, e.g., [22].

Parameter-dependent multiplier

The most computationally expensive multiplier considered in this work is the parameter-dependent multiplier which is an affine function of the parameter vector p.

$$\Pi(p) = \left[\begin{array}{cc} \tilde{S}_0^\top \Delta + \Delta^\top \tilde{S}_0 & -\tilde{S}_0^\top - \Delta^\top \tilde{S}_1^\top \\ -\tilde{S}_0 - \tilde{S}_1 \Delta & \tilde{S}_1 + \tilde{S}_1^\top \end{array}\right], \quad (15)$$

where S_0 and S_1 are of appropriate dimensions. By substituting this multiplier into (10), it can be seen that the constraint is equal to $0 \ \forall p \in \mathcal{P}$, so the constraint is automatically fulfilled. The complexity of using this multiplier arises in that (9) is now parameter-dependent. Since $\Pi(p)$ is an affine function of p which is constrained to a polytope, checking (9) only at the vertices of $\mathcal{P}$ implies that it holds $\forall p \in \mathcal{P}$. This results in 2^{n_δ} LMIs, one for each vertex of $\mathcal{P}$.

For all applications of the full block S-Procedure in this paper, multipliers are restricted to one of the three forms described in this section.

B. Coprime Factorisation

Consider an LPV system P as described in (1). A contractive left-coprime factorisation of the system $P = M^{-1}N$ provides a kernel representation of all stable input-output pairs [23]–[25]. By definition, $y = M^{-1}Nu$, thus $0 = [M, -N][y^\top, u^\top]^\top$, so the set of all input-output pairs is characterised by the null space of $[M, -N]$. In order to be contractive, the factorisation must also satisfy $\|[M, N]\| \leq 1$.

A state-space representation of $[M, N]$ for an LPV plant (1) is

$$\left[\begin{array}{c} \dot{\mu} \\ \hline v \end{array}\right] = \left[\begin{array}{c|cc} A + LC & L & B + LD \\ \hline R^{-\frac{1}{2}} C & R^{-\frac{1}{2}} & R^{-\frac{1}{2}} D \end{array}\right] \left[\begin{array}{c} \mu \\ \hline y \\ -u \end{array}\right], \quad (16)$$

(*dependency on ρ is omitted from (16) for brevity*) where $L(\rho)$ is a filter gain matrix and $R(\rho) := I + D(\rho)D^\top(\rho)$.

The conditions of the contractive left-coprime factorisation can be derived by applying a generalisation of the BRL (Theorem 1) to the state-space realisation of the coprime factorisation (16). This was proven in the thesis of Wood [25].

III. Two-Step Controller Synthesis for LPV Systems

When finding an optimal output-feedback controller using induced $\mathcal{L}_2$ synthesis, the SDP is made up of a generalised filtering algebraic Ricatti inequality and a generalised control algebraic Ricatti inequality [26]. In this section, the output-feedback synthesis problem is separated into two smaller SDPs; namely a filter gain ($L(\rho)$) synthesis and a state-feedback gain ($F(\rho)$) synthesis. Hence, the presented structured approach is more computationally efficient than an equivalent output-feedback controller synthesis. The system and resulting structured controller are formulated using the

LFT framework. Consider an LPV plant with the following state-space realisation

$$\left[\begin{array}{c} \dot{x} \\ \hline y \end{array}\right] = \left[\begin{array}{c|c} A(\rho) & B(\rho) \\ \hline C(\rho) & 0 \end{array}\right] \left[\begin{array}{c} x \\ \hline u+d \end{array}\right], \tag{17}$$

which is equivalent to (1) except that $D(\rho) = 0$ and the input has a summative disturbance d. For the sake of brevity in this paper, the plant is assumed to be strictly proper. This assumption is not restrictive as many practical problems can be accurately described with this representation by augmenting the system (e.g., with actuator dynamics, which removes the direct feed-through from u to y). Alternatively, a loop-shifting transformation [27] can be applied $y \leftarrow y^{(1)} + Du$ which results in a strictly proper plant and a controller with an additional feedback loop of $-D$ to maintain the closed-loop properties. The following results can be reproduced for more general plants with $D(\rho) \neq 0$, at the expense of more complicated formulae.

The controller K calculates the command signal u from an error signal $e = r - y$, where r is some reference value for the output y. The controller is designed such that it meets specific requirements, by establishing a bound on the induced $\mathcal{L}_2$-norm of the closed-loop interconnections of an augmented plant P_{aug} and K, as described in Section II. These requirements can be, for example, disturbance attenuation levels, tracking capabilities, the frequency range of control activity and robustness. P_{aug} is designed by augmenting the in/outputs of P with dynamic weights. The weighting structure used in this paper is a mixed-sensitivity structure developed by Theis et al. [13] that has been applied to many use-cases in aerospace [2], [28]. Although the plant is LPV, the weighting structure in most cases can be linear time-invariant (LTI) since, in many controls problems, performance specifications remain consistent across the parameter space and therefore do not depend on the scheduling parameter. To maintain generality, an LPV weighting scheme is used for the derivation of the remaining theory. Equivalent formulations exist for LPV or LTI weights and the derivations in this paper apply in both cases. Defining the output sensitivity function $S = (I + PK)^{-1}$, the generalised closed-loop of the weighted problem is

$$F_l(P_{aug}, K) : \begin{bmatrix} z_1 \\ z_2 \end{bmatrix} = \begin{bmatrix} W_e V_e^{-1} & 0 \\ 0 & W_u V_u^{-1} \end{bmatrix} \underbrace{\begin{bmatrix} S & -SP \\ KS & -KSP \end{bmatrix}}_{\text{4 blocks}} \begin{bmatrix} V_e & 0 \\ 0 & V_d \end{bmatrix} \begin{bmatrix} w_1 \\ w_2 \end{bmatrix}, \tag{18}$$

where W_e and W_u denote parameter-dependent dynamic weights, with state-space formulation as in (1), and $V_e(\rho)$, $V_u(\rho)$, and $V_d(\rho)$ are parameter-dependent scaling factors. This is described as the four-block mixed-sensitivity synthesis problem as it shapes four unique closed-loop transfer functions. Increasing the magnitude of W_e reduces the sensitivity function which leads to better tracking and disturbance rejection. In most applications W_e will have high magnitude at low frequency and a high frequency gain of -6 dB to keep the peak of the sensitivity function below 2. Consequently, this also imposes the shape of the complementary sensitivity function $(I - S)$, so the tracking bandwidth imposed by W_e also influences the frequency content of attenuated noise on the output. Increasing the magnitude of W_u can be used to limit the frequency of the commanded actuation according to the available bandwidth and to avoid excitation of flexible modes in a system. Typically, W_u has high magnitude in the frequency range outside of the desired control activity, and hence causes a roll-off in the controller. The static scalings are used as the main tuning parameters. Good initial values are based on the expected values of the signals in the system. These correspond to the maximum allowable errors ($V_e(\rho)$), the maximum allowable commands ($V_u(\rho)$), and the maximum expected disturbances ($V_d(\rho)$). Theis et al. [13] present a comprehensive treatment of this parameterisation for an LTI weighting scheme.

The goal of the proposed synthesis framework is to separate the controller synthesis into two steps such that the mixed-sensitivity output-feedback problem is solved in two stages. A filter problem is solved first, followed by a state-feedback gain calculation. The proposed filter O, with gain $L(\rho)$, and controller gain $F(\rho)$ are connected with the presented weighting scheme as in the block diagram shown in Figure 1.

To understand the two synthesis stages, first, the performance of the output-feedback problem is defined by the induced $\mathcal{L}_2$-norm of its generalised weighted closed-loop interconnections (18)

$$\|F_l(P_{aug}, K)\| = \left\| \begin{bmatrix} W_e V_e^{-1} & 0 \\ 0 & W_u V_u^{-1} \end{bmatrix} \begin{bmatrix} S & -SP \\ KS & -KSP \end{bmatrix} \begin{bmatrix} V_e & 0 \\ 0 & V_d \end{bmatrix} \right\|, \tag{19}$$

with the dependency on ρ omitted from the notation. Consider the plant has a contractive left-coprime factorisation $P = M^{-1}N$. An equivalent two-block problem with input weight M^{-1}, from the factorisation, can be defined. Substituting P for its coprime factorisation $M^{-1}N$ and considering that by definition $\|[M,\ N]\| \leq 1$, it follows from the sub-multiplicativity of the $\mathcal{L}_2$-norm that the norm of the proposed synthesis problem (Figure 2) is bounding the norm of the original problem.

$$\underbrace{\left\| \begin{bmatrix} W_e V_e^{-1} & 0 \\ 0 & W_u V_u^{-1} \end{bmatrix} \begin{bmatrix} S \\ KS \end{bmatrix} M^{-1} \begin{bmatrix} M & -N \end{bmatrix} \begin{bmatrix} V_e & 0 \\ 0 & V_d \end{bmatrix} \right\|}_{\text{proposed } \|F_l(P_{aug},K)\|} \leq \left\| \begin{bmatrix} W_e V_e^{-1} & 0 \\ 0 & W_u V_u^{-1} \end{bmatrix} \begin{bmatrix} S \\ KS \end{bmatrix} M^{-1} \begin{bmatrix} V_e \end{bmatrix} \right\|. \tag{20}$$

Hence, a controller that minimises the induced $\mathcal{L}_2$-norm on the right-hand side of (20), upper bounds the performance of the original problem (19) (Figure 1). The severity of the conservatism introduced to the solution depends on $\|[M,\ N]\|$. Magnitudes closer to one yield less conservatism.

By restricting the structure of K to a structured, filter-based controller K_S, the two-block mixed-sensitivity problem becomes a state-feedback problem with a filter. The state-space

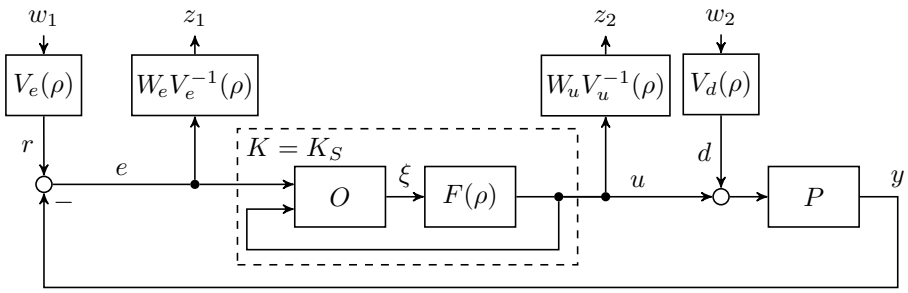

Fig. 1. Closed-loop interconnection of plant, controller and mixed-sensitivity weighting scheme.

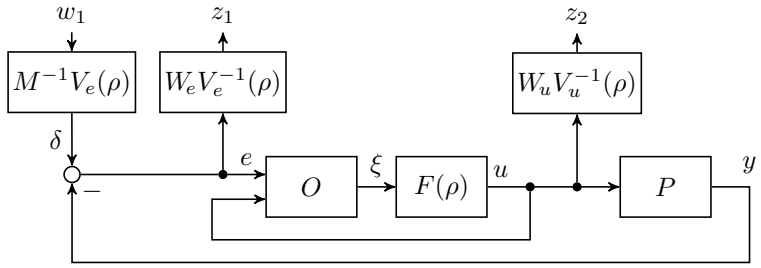

Fig. 2. Closed-loop two-block mixed-sensitivity problem.

formulation of the filter is

$$O : \left[\begin{array}{c}\dot{\xi}\\ \hline \xi\end{array}\right] = \left[\begin{array}{c|cc} A(\rho)+L(\rho)C(\rho) & L(\rho) & B(\rho) \\ \hline I & 0 & 0\end{array}\right]\left[\begin{array}{c}\xi\\ \hline e\\ u\end{array}\right], \tag{21}$$

where $L(\rho)$ is the parameter-varying filter gain and ξ is the estimated states. The control law is

$$u = F(\rho)\xi. \tag{22}$$

Therefore, the state-space formulation of the combined structured controller is

$$K_S : \left[\begin{array}{c}\dot{\xi}\\ \hline u\end{array}\right] = \left[\begin{array}{c|c} A+BF+LC & L \\ \hline F & 0\end{array}\right]\left[\begin{array}{c}\xi\\ \hline e\end{array}\right]. \tag{23}$$

As it will be shown in this section, by intentionally choosing the filter gain $L(\rho)$ to be equal to the solution of the contractive left-coprime factorisation, the filter-based control problem converges to the output-feedback problem. In other words, the filter is optimal, and therefore the conservatism is minimised. Thus, the synthesised controller for the two-block problem is an optimal controller in an induced $\mathcal{L}_2$-norm sense.

It will now be demonstrated that, for the derived two-block problem to be solved in (20), the filter and state-feedback controller are uni-directionally coupled. This means that the performance of the filter is independent from the controller gain, so it can easily be computed first. Following this is the derivation of the state-feedback problem.

The proposed filter (21) has a similar structure to a state observer, however it does not estimate the plant states but provides the estimated error states ξ, such that $C(\rho)\xi$ is the estimated error. Consider the difference between the estimated error and the true error as a performance metric of the filter, denoted $\hat{e}$

$$\hat{e} = \underbrace{C(\rho)\xi}_{\text{estimated error}} - \underbrace{(y-r)}_{\text{true error}} = C(\rho)\xi + e \tag{24}$$

$\hat{e}$ shall be referred to as the estimation error, not to be confused with the *estimated* error. It will now be shown that the estimation error is independent from the state-feedback gains $F(\rho)$. Consequently, the filter and state-feedback gains are coupled in only one direction; $F(\rho)$ depends on $L(\rho)$ but $L(\rho)$ does not depend on $F(\rho)$. This is an important demonstration of how the overall controller design problem can be separated into a filter and a state-feedback design. The closed-loop is derived by first combining (23) and (17)

$$\left[\begin{array}{c}\dot{x}\\ \dot{\xi}\\ \hline y\end{array}\right] = \left[\begin{array}{cc|cc} A & BF & 0 & B \\ -LC & A+LC+BF & L & 0 \\ \hline C & 0 & 0 & 0\end{array}\right]\left[\begin{array}{c}x\\ \xi\\ \hline r\\ d\end{array}\right]. \tag{25}$$

Then, the estimation error $\hat{e}$ is introduced as an output instead of y.

$$\left[\begin{array}{c}\dot{x}\\ \dot{\xi}\\ \hline \hat{e}\end{array}\right] = \left[\begin{array}{cc|cc} A & BF & 0 & B \\ -LC & A+LC+BF & L & 0 \\ \hline -C & C & I & 0\end{array}\right]\left[\begin{array}{c}x\\ \xi\\ \hline r\\ d\end{array}\right]. \tag{26}$$

By defining a new state $\epsilon = \xi - x$ and completing a coordinate transformation

$$\left[\begin{array}{c}\dot{\epsilon}\\ \dot{\xi}\\ \hline \hat{e}\end{array}\right] = \left[\begin{array}{cc|cc} A+LC & 0 & L & -B \\ LC & A+BF & L & 0 \\ \hline C & 0 & I & 0\end{array}\right]\left[\begin{array}{c}\epsilon\\ \xi\\ \hline r\\ d\end{array}\right], \tag{27}$$

ξ is shown to be unobservable from the performance metric $\hat{e}$ and can be removed as a state. The final state-space formulation is

$$\left[\begin{array}{c}\dot{\epsilon}\\ \hline \hat{e}\end{array}\right] = \left[\begin{array}{c|cc} A+LC & L & B \\ \hline C & I & 0\end{array}\right]\left[\begin{array}{c}\epsilon\\ \hline r\\ -d\end{array}\right]. \tag{28}$$

From (28), $F(\rho)$ has no influence on $\hat{e}$, the filter can be synthesised without any knowledge of the controller as its performance is independent from the state-feedback gain. It is also now clear that (28) represents the performance of the filter (output $\hat{e}$) with respect to the disturbance dynamics of the plant, i.e., response to input d. Notice that (28) has the same formulation as the state-space realisation of the coprime factorisation (16) for the disturbance dynamics of the plant (17). Therefore, the optimal filter gain is chosen as $L(\rho)$ when solving the contractive left-coprime factorisation of the *disturbance plant*, scaled with respect to the mixed-sensitivity weighting structure. Thus, for the weighting scheme presented in this paper, the $V_e(\rho)$ and $V_d(\rho)$ scalings must be considered.

Having established the uni-directional coupling between $L(\rho)$ and $F(\rho)$, now it remains to fully derive the two-block state-feedback problem (Figure 2) with respect to the original output-feedback problem and mixed-sensitivity weighting structure (Figure 1). The equivalency of (16) and (28) means that the estimation error can also be defined as $\hat{e} = Mr - Nd$. Hence a new input signal to the two-block problem is defined $\delta = r - M^{-1}Nd$. This is equivalent to $\delta = r - Pd$. Thus, it characterises the reference signal and disturbance dynamics of the plant in the mixed-sensitivity design. By taking the inverse of M from the coprime factorisation (16), the input weight for the two-block problem is defined as

$$M^{-1}: \left[\begin{array}{c}\dot{\alpha}\\ \hline \delta\end{array}\right] = \left[\begin{array}{c|c} A(\rho) & L(\rho) \\ \hline -C(\rho) & I\end{array}\right]\left[\begin{array}{c}\alpha\\ \hline \hat{e}\end{array}\right]. \tag{29}$$

It shall be emphasised that the same gain $L(\rho)$ appears in M^{-1} and the filter O.

The state-space formulation of the interconnection of M^{-1}, O, and P, given that $\hat{e} = C(\rho)\xi + e$, is

$$\left[\begin{array}{c}\dot{x}\\ \dot{\xi}\\ \dot{\alpha}\\ \hline e\\ u\\ \xi\end{array}\right] = \left[\begin{array}{ccc|cc} A(\rho) & 0 & 0 & 0 & B(\rho) \\ 0 & A(\rho) & 0 & L(\rho) & B(\rho) \\ 0 & 0 & A(\rho) & L(\rho) & 0 \\ \hline 0 & -C(\rho) & 0 & I & 0 \\ 0 & 0 & 0 & 0 & I \\ 0 & I & 0 & 0 & 0\end{array}\right]\left[\begin{array}{c}x\\ \xi\\ \alpha\\ \hline \hat{e}\\ u\end{array}\right], \tag{30}$$

where ξ are estimated error states that feed into the controller $F(\rho)$. The control error e and control command u are the performance outputs for the mixed-sensitivity synthesis. Notice that neither x nor α are observed in the outputs, so both states can be eliminated to form an equivalent, minimal realisation

$$\left[\begin{array}{c}\dot{\xi}\\ \hline e\\ u\\ \xi\end{array}\right] = \left[\begin{array}{c|cc} A(\rho) & L(\rho) & B(\rho) \\ \hline -C(\rho) & I & 0 \\ 0 & 0 & I \\ I & 0 & 0\end{array}\right]\left[\begin{array}{c}\xi\\ \hline \hat{e}\\ u\end{array}\right]. \tag{31}$$

Equation (31) now forms the open-loop plant P in the induced $\mathcal{L}_2$-norm state-feedback problem to be solved.

Next, the plant is augmented to form P_{aug} such that K is synthesised based on the performance requirements imposed by the weighting structure. The mixed-sensitivity static and dynamic weights are added to the open-loop system (as per Figure 2). The dynamic weights are denoted as state-space systems

$$W_1 = W_e V_e^{-1}(\rho),\ W_2 = W_u V_u^{-1}(\rho) \tag{32a}$$

$$W_1: \left[\begin{array}{c}\dot{\xi}_1\\ \hline z_1\end{array}\right] = \left[\begin{array}{c|c} A_1(\rho) & B_1(\rho) \\ \hline C_1(\rho) & D_1(\rho)\end{array}\right]\left[\begin{array}{c}\xi_1\\ \hline e\end{array}\right], \tag{32b}$$

$$W_2: \left[\begin{array}{c}\dot{\xi}_2\\ \hline z_2\end{array}\right] = \left[\begin{array}{c|c} A_2(\rho) & B_2(\rho) \\ \hline C_2(\rho) & D_2(\rho)\end{array}\right]\left[\begin{array}{c}\xi_2\\ \hline u\end{array}\right], \tag{32c}$$

so additional states ξ_1 and ξ_2 are introduced to the system. Given the (already known) relationship $\hat{e} = C(\rho)\xi + e$, the output weights (32) are connected to the open-loop state-space system (31), resulting in the following state-space realisation (with dependency on ρ omitted from this point in the derivation)

$$\left[\begin{array}{c}\dot{\xi}\\ \dot{\xi}_1\\ \dot{\xi}_2\\ \hline z_1\\ z_2\\ \xi\end{array}\right] = \left[\begin{array}{ccc|cc} A & 0 & 0 & L & B \\ -B_1C & A_1 & 0 & B_1 & 0 \\ 0 & 0 & A_2 & 0 & B_2 \\ \hline -D_1C & C_1 & 0 & D_1 & 0 \\ 0 & 0 & C_2 & 0 & D_2 \\ I & 0 & 0 & 0 & 0\end{array}\right]\left[\begin{array}{c}\xi\\ \xi_1\\ \xi_2\\ \hline \hat{e}\\ u\end{array}\right]. \tag{33}$$

Then, from (29), the scaled input w_1 is defined as $w_1 = V_e(\rho)\hat{e}$. Additionally, the control signal u is scaled to $u_{sc} = D_2(\rho)u$ (i.e. with the same factor as z_2) such that the overall synthesis results in a scaled controller. Finally, adding the dynamic weight states ξ_1 and ξ_2 to the controller inputs maintains the state-feedback structure. The resulting mixed-sensitivity weighted plant for the state-feedback controller synthesis is therefore

$$\left[\begin{array}{c}\dot{\xi}\\ \dot{\xi}_1\\ \dot{\xi}_2\\ \hline z_1\\ z_2\\ \xi\\ \xi_1\\ \xi_2\end{array}\right] = \left[\begin{array}{ccc|cc} A & 0 & 0 & LV_e & BD_2^{-1} \\ -B_1C & A_1 & 0 & B_1V_e & 0 \\ 0 & 0 & A_2 & 0 & B_2D_2^{-1} \\ \hline -D_1C & C_1 & 0 & D_1V_e & 0 \\ 0 & 0 & C_2 & 0 & I \\ I & 0 & 0 & 0 & 0 \\ 0 & I & 0 & 0 & 0 \\ 0 & 0 & I & 0 & 0\end{array}\right]\left[\begin{array}{c}\xi\\ \xi_1\\ \xi_2\\ \hline w_1\\ u_{sc}\end{array}\right]. \tag{34}$$

By minimising the induced $\mathcal{L}_2$-norm of the closed-loop interconnection of this weighted plant and the controller, the optimal controller gain is determined (the synthesis is detailed in a later section). Note that the output from the synthesised controller is a scaled signal u_{sc}. Therefore, the scaling of the synthesised gain $F_{sc}(\rho)$ must be reversed before implementing in the closed-loop system; $F(\rho) = D_2^{-1}(\rho)F_{sc}(\rho)$.

The following proposition is made to concisely summarise the findings of Theis and Pfifer [29] which were reiterated in this section. This is later developed into a novel LFT-based controller synthesis.

Proposition 1. The mixed-sensitivity problem (Figure 1) can be solved more efficiently by separating the filter and state-feedback synthesis. The optimal filter gain is calculated from

the solution of the contractive left-coprime factorisation of the plant's disturbance dynamics. This transforms the mixed-sensitivity problem into a two block state-feedback problem. This filter gain guarantees that the $\mathcal{L}_2$ performance of the original output-feedback problem is upper bounded by the $\mathcal{L}_2$ performance of the two-block state-feedback problem. The resulting structured controller takes the form in (23).

A. Resulting Structured Controller

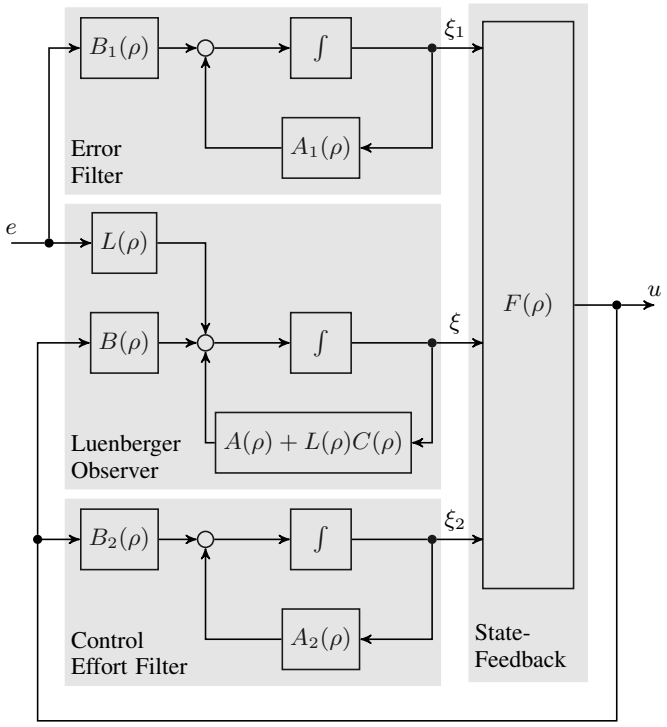

Fig. 3. Final controller structure of K_S.

This section demonstrates that the proposed controller design results in a highly structured controller K_S. From (34), the additional states ξ_1 and ξ_2 from the weighting scheme are included in the controller formulation (23)

$$\begin{bmatrix} \dot{\xi} \\ \dot{\xi}_1 \\ \dot{\xi}_2 \\ \hline u \end{bmatrix} = \left[\begin{array}{ccc|c} & A_{K_S} & & \begin{matrix} L \\ B_1 \\ 0 \end{matrix} \\ \hline F_{11} & F_{12} & F_{13} & 0 \end{array}\right] \begin{bmatrix} \xi \\ \xi_1 \\ \xi_2 \\ \hline e \end{bmatrix},$$

where

$$A_{K_S} = \begin{bmatrix} A + LC + BF_{11} & BF_{12} & BF_{13} \\ 0 & A_1 & 0 \\ B_2F_{11} & B_2F_{12} & A_2 + B_2F_{13} \end{bmatrix}. \tag{35}$$

By separating the three sets of states ξ, ξ_1, ξ_2, the control structure is split into three existing, well-known parts

$$\begin{aligned} &\text{Luenberger Observer:} && \dot{\xi} = A\xi + L\underbrace{V_e w_1}_{C\xi+e} + B\underbrace{D_2^{-1}w_2}_{u} \\ &\text{Error Filter:} && \dot{\xi}_1 = A_1\xi_1 - B_1\underbrace{C\xi}_{\hat{e}-e} + B_1\underbrace{V_e w_1}_{\hat{e}} \\ &\text{Control Effort Filter:} && \dot{\xi}_2 = A_2\xi_2 + B_2\underbrace{D_2^{-1}w_2}_{u} \end{aligned} \tag{36}$$

The resulting structure, as depicted in Figure 3, ensures the controller is straightforward to implement. It is common that $A_1 = I$, thus the *Error Filter* will provide integral action. With the given structure, the integrators in this case are separated which allows for easier implementation of anti-windup schemes. Another benefit of the presented structured design is that the design weights do not have to be strictly stable, as they would in traditional output-feedback control [30], [31]. In the presented state-feedback problem, the states include those from the design weights ξ_1 and ξ_2, thus the weights can be stabilised in the closed-loop.

B. Filter Synthesis

As described, the filter gain $L(\rho)$ is calculated from the contractive left-coprime factorisation of the scaled disturbance dynamics of the plant. The plant is first scaled by $P_{sc} = V_e^{-1}(\rho)PV_d(\rho)$, where P is given in (17) and $V_e(\rho)$ and $V_d(\rho)$ are based on the maximum allowable errors and maximum allowable disturbance, respectively. In order to make the coprime factorisation computationally tractable for the LPV plant in LFT form, the LMIs are transformed to eliminate the dependence on ρ from the computation by using the full block S-Procedure (Theorem 2). First, the left-coprime factorisation of P_{sc} is calculated, as described in Section II-B. The conditions are summarised in the following theorem.

Theorem 3. Given the scaled LPV plant P_{sc}, there exists a contractive left-coprime factorisation $P_{sc} = M_{sc}^{-1}N_{sc}$ if there exists a continuously differentiable, symmetric matrix function $Z(p) : \mathcal{P} \to \mathbb{R}^{n_x \times n_x}$ such that $\forall (p, q) \in \mathcal{P} \times \dot{\mathcal{P}}$

$$Z > 0 \tag{37a}$$

$$\begin{bmatrix} \partial Z + ZA_{sc} + A_{sc}^\top Z - C_{sc}^\top C_{sc} & ZB_{sc} \\ B_{sc}^\top Z & -I \end{bmatrix} < 0 \tag{37b}$$

Proof. The proof is based on applying a generalisation of the BRL (Theorem 1) to the state-space realisation of the coprime factorisation (28) and is provided in the thesis of Wood [25].

The resulting filter gain is calculated from the storage function and plant matrices as $L_{sc}(p) = -Z^{-1}(p)C_{sc}^\top(p)$. To reverse the scaling for implementation in the closed-loop, $L(p) = L_{sc}(p)V_e^{-1}(p)$. By finding the filter gain that minimises trace$(Z^{-1}(p))$, the solution to the structured control problem converges to the solution of the equivalent state-feedback problem (assuming the states are measurable). Thus, $L(p)$ converges to the optimal filter gain and the conservatism introduced by the filter is minimised. For a full explanation, refer to the work of Theis and Pfifer [14]. Considering that $Z(p)$ is a continuous function of p in a compact set, then

$Z(0) > 0$ and (37b) imply (37a). Therefore (37a) can be replaced by $Z(0) > 0$. The second LMI (37b) requires further reformulation steps before applying the full block S-Procedure. First, it must be transformed into a quadratic expression with LFTs as outer factors. The parameter dependency of (37b) is factorised in two steps. The initial factorisation separates the parameter-dependent matrices from all $Z(p)$ terms

$$\left[\begin{array}{c|c} * & \end{array}\right]^\top \left[\begin{array}{cc|cc} 0 & Z & & \\ Z & \partial Z & & \\ \hline & & -I & 0 \\ & & 0 & -I \end{array}\right] \left[\begin{array}{cc} A_{sc} & B_{sc} \\ I & 0 \\ -C_{sc} & 0 \\ 0 & -I \end{array}\right] < 0. \tag{38}$$

To reduce notation, throughout this paper $*$ represents symmetry that maintains a quadratic structure. Also, zero, off-diagonal blocks are generally omitted. Then the structure of $Z(p)$ is itself restricted to a quadratic form $Z(p) = G^\top(p) Z_0 G(p)$. Consequently, $\partial Z(p,q) = \partial G^\top(p,q) Z_0 G(p) + G^\top(p) Z_0 \partial G(p,q)$. The matrix $G(p)$ describes the parameter dependency of the system and must be a rational function that satisfies the quadratic structure of $Z(p)$. A common choice is to use an even-ordered polynomial, such that

$$\begin{aligned} Z(p) &= \left[\begin{array}{c|c} * & \end{array}\right]^\top \underbrace{\left[\begin{array}{ccc} Z_{0,11} & Z_{0,12} & \cdots & Z_{0,1n} \\ Z_{0,21} & \ddots & & \vdots \\ \vdots & & \ddots & \vdots \\ Z_{0,n1} & \cdots & \cdots & Z_{0,nn} \end{array}\right]}_{Z_0} \underbrace{\left[\begin{array}{c} I \\ pI \\ \vdots \\ p^{n-1} \end{array}\right]}_{G(p)} \\ &= \sum_{n=1}^{k} \left(p^{n-1} \sum_{m=1}^{k} Z_{0,nm} p^{m-1} \right), \end{aligned} \tag{39}$$

where $2(k-1)$ is the order and k is an integer. Note also that $Z_{0,nm} = Z_{0,mn}^\top$ due to symmetry. For example, a second-order parameter dependency would result in $Z(p) = Z_{0,11} + p(Z_{0,12} + Z_{0,12}^\top) + p^2 Z_{0,22}$.

Now that the structure of $Z(p)$ is restricted, the second step of the factorisation is to separate the remaining parameter-dependent terms into the outer factors. In this way, all dependency on p is removed from the central term.

Then (38) is equivalent to

$$\left[\begin{array}{c|c} * & \end{array}\right]^\top \underbrace{\left[\begin{array}{cc|cc} 0 & Z_0 & & \\ Z_0 & 0 & & \\ \hline & & -I & 0 \\ & & 0 & -I \end{array}\right]}_{Z_{0,mat}} \underbrace{\left[\begin{array}{cc} GA_{sc} + \partial G & GB_{sc} \\ G & 0 \\ C_{sc} & 0 \\ 0 & I \end{array}\right]}_{Q_z(p,q)} < 0. \tag{40}$$

The infinite dimensional LMI (37b) is now an inequality with the quadratic form ${Q_z}^\top(p,q) Z_{0,mat} Q_z(p,q) < 0$. The outer factor $Q_z(p,q)$ can be cast into an upper LFT with partitioned matrix $Q_{z,0}$, as described in (3). This can be done with readily available tools, such as `lftdata` in the Robust Control Toolbox in MATLAB. Then, the full block S-Procedure is applied with a multiplier Π_{Q_z} which is restricted to a structure specified in Section II-A to handle the parameter dependency from the conditions of Theorem 3. As a result, it is proven that the quadratic matrix inequality ${Q_z}^\top(p,q) Z_{0,mat} Q_z(p,q) < 0$ with $Z_0 \in \mathbb{S}^{n_2 \times n_2}$, holds for all $p, q \in \mathcal{P} \times \dot{\mathcal{P}}$ if and only if there exists a full block multiplier $\Pi_{Q_z} \in \mathbb{S}^{(n_1+m_1)\times(n_1+m_1)}$ as defined in Section II-A such that

$$Z_0 > 0 \tag{41a}$$

$$G(0)^\top Z_0 G(0) > 0 \tag{41b}$$

$$\left[\begin{array}{c|c} * & \end{array}\right]^\top \left[\begin{array}{c|c} \Pi_{Q_z} & \\ \hline & Z_{0,mat} \end{array}\right] \left[\begin{array}{cc|cc} Q_{z,11} & Q_{z,12} & & \\ I & 0 & & \\ \hline & & Q_{z,21} & Q_{z,22} \end{array}\right] < 0. \tag{41c}$$

The optimal filter gain is achieved by minimising $\text{trace}(Z^{-1}(p))$ under the conditions of Theorem 3, now transformed into equations (41). In order to minimise the trace of an inverted variable, an additional slack variable $U(p) \in \mathbb{R}^{n_x \times n_x}$ must be introduced such that $\text{trace}(U(p)) > \text{trace}(Z^{-1}(p))$. This is achieved with the added constraint

$$\left[\begin{array}{cc} U(p) & I \\ I & Z(p) \end{array}\right] > 0 \ \forall p \in \mathcal{P}. \tag{42}$$

A slightly reduced condition can be formulated with a static U, however this may result in additional conservatism on the controller's performance. Equation (42) is then factorised and transformed with the full block S-Procedure. First $U(p)$ is restricted to $G^\top(p) U_0 G(p)$, so, the factorisation of (42) is

$$\left[\begin{array}{c|c} * & \end{array}\right]^\top \underbrace{\left[\begin{array}{ccc|c} U_0 & & & \\ & 0 & I & \\ & I & 0 & \\ \hline & & & Z_0 \end{array}\right]}_{U_{mat}} \underbrace{\left[\begin{array}{cc} G & 0 \\ 0 & I \\ I & 0 \\ 0 & G \end{array}\right]}_{Q_w(p)} > 0. \tag{43}$$

Then, as with $Q_z(p,q)$ from (40) to (41), the outer factor $Q_w(p)$ is cast into an upper LFT with partitioned matrix $Q_{w,0}$. Then the full block S-Procedure is applied with a full block multiplier Π_{Q_w}, which is also restricted to a structure in Section II-A. Thus, condition (42) is equivalent to

$$\left[\begin{array}{c|c} * & \end{array}\right]^\top \left[\begin{array}{c|c} \Pi_{Q_w} & \\ \hline & U_{mat} \end{array}\right] \left[\begin{array}{cc|cc} Q_{w,11} & Q_{w,12} & & \\ I & 0 & & \\ \hline & & Q_{w,21} & Q_{w,22} \end{array}\right] > 0. \tag{44}$$

Combining the derivations so far, there is a fully solvable existence condition for the coprime factorisation of the disturbance dynamics of an LFT-based LPV plant (17) scaled with respect to the weighting structure in Figure 1. These conditions are given in Corollary 1.

Corollary 1. Let $\mathcal{P}$ be a given compact set and P_{sc} a scaled LPV plant (17). There exists a contractive left-coprime factorisation $P_{sc} = M_{sc}^{-1} N_{sc}$ if there exist continuously differentiable, symmetric matrix functions $Z : \mathcal{P} \to \mathbb{R}^{n_x \times n_x}$ and $U : \mathcal{P} \to \mathbb{R}^{n_x \times n_x}$ where $Z(p)$ and $U(p)$ are restricted to quadratic

structures $Z(p) = G^\top(p) Z_0 G(p)$, $U(p) = G^\top(p) U_0 G(p)$, and $G(p)$ is rational, such that $\forall p \in \mathcal{P}$

$$Z_0 > 0 \tag{45a}$$

$$G(0)^\top Z_0 G(0) > 0 \tag{45b}$$

$$\left[\begin{array}{c|c} * & * \end{array}\right]^\top \left[\begin{array}{c|c} \Pi_{Q_z} & \\ \hline & Z_{0,mat} \end{array}\right] \left[\begin{array}{cc} Q_{z,11} & Q_{z,12} \\ I & 0 \\ \hline Q_{z,21} & Q_{z,22} \end{array}\right] < 0 \tag{45c}$$

$$\left[\begin{array}{c|c} * & * \end{array}\right]^\top \left[\begin{array}{c|c} \Pi_{Q_w} & \\ \hline & U_{mat} \end{array}\right] \left[\begin{array}{cc} Q_{w,11} & Q_{w,12} \\ I & 0 \\ \hline Q_{w,21} & Q_{w,22} \end{array}\right] > 0, \tag{45d}$$

where $Z_{0,mat}$ and U_{mat} take the forms derived in (40) and (43). $Q_{z,0}$, $Q_{w,0}$ are partitioned upper LFT matrices, from the definitions of $Q_z(p)$ and $Q_w(p)$ in (40) and (43). The multipliers Π_{Q_z} and Π_{Q_w} are symmetric and are restricted to a structure as in Section II-A.

The optimal scaled filter gain is calculated by minimising trace$(U(p))$ with respect to the existence conditions in Corollary 1. Then the un-scaled gain, for implementation in the closed-loop system is calculated as $L(p) = -Z^{-1}(p) C_{sc}^\top(p) V_e^{-1}(\rho)$.

C. State-Feedback Synthesis

In this section, the state-feedback step of the structured controller synthesis is presented. A state-feedback controller is synthesised for the LFT-based generalised plant P_{SF} with weighting structure in (34). Then, as with the filter synthesis, the existence conditions are transformed using the full block S-Procedure (Theorem 2) so that the proposed optimisation is computationally solvable. As per (20), the state-feedback synthesis provides an upper bound on the performance of the original output-feedback problem. The conservatism of the bound depends on the norm of the coprime factorisation $\|[M,\ N]\|$. A reduced notation for the generalised plant (34) that is used in this section is

$$P_{\text{SF}} : \left[\begin{array}{c} \dot{x} \\ \hline z_1 \\ z_2 \\ x \end{array}\right] = \left[\begin{array}{c|cc} \bar{A} & \bar{B}_{11} & \bar{B}_{12} \\ \hline \bar{C}_1 & \bar{D}_1 & 0 \\ \bar{C}_2 & 0 & I \\ I & 0 & 0 \end{array}\right] \left[\begin{array}{c} x \\ \hline w_1 \\ u_{sc} \end{array}\right], \tag{46}$$

with the scaled command u_{sc} as the output of the synthesised controller and the states x (equivalent to $[\xi^\top,\ \xi_1^\top,\ \xi_2^\top]^\top$ in (34)) as the input. The following theorem states the conditions for the synthesis of a state-feedback controller for the open-loop plant (46).

Theorem 4. Let $\mathcal{P}$ be a given compact set and P_{SF} an LPV system as in (46) with measurable states x. There exists a stabilising state-feedback control law $F_{sc} : u_{sc} = F_{sc}(\rho) x$ such that $\|F_l(P_{\text{SF}}, F_{sc}(\rho))\| \leq \gamma$, where γ is a constant $\gamma > \bar{\sigma}(\bar{D}_1)$, if there exists a continuously differentiable, symmetric matrix function $Y : \mathcal{P} \to \mathbb{R}^{n_x \times n_x}$ such that $\forall (p, q) \in \mathcal{P} \times \dot{\mathcal{P}}$

$$Y > 0 \tag{47a}$$

$$\left[\begin{array}{ccc} Y\hat{A}^\top + \hat{A}Y - \partial Y - \gamma \bar{B}_{12}\bar{B}_{12}^\top & Y\bar{C}_1^\top & \bar{B}_{11} \\ \bar{C}_1 Y & -\gamma I & \bar{D}_1 \\ \bar{B}_{11}^\top & \bar{D}_1^\top & -\gamma I \end{array}\right] < 0, \tag{47b}$$

where $\hat{A}(p) := \bar{A}(p) - \bar{B}_{12}(p)\bar{C}_2(\rho)$
Then the state-feedback gain can be calculated from the open-loop plant matrices and the feasible values of $Y(p)$ and γ as $F_{sc}(p) = \gamma \bar{B}_{12}^\top(p) Y(p)^{-1} + \bar{C}_2(\rho)$.

Proof. The derivation and proof of these conditions are provided in the thesis of Wu [20].

Now, much like for the filter synthesis (Section III-B), the existence conditions are transformed to be computationally solvable. First, inequality (47a) is replaced with $Y(0) > 0$, following the same reasoning as for inequality (37a). Then, to reformulate (47b), the structure of $Y(p)$ is restricted to $Y(p) = H^\top(p) Y_0 H(p)$, which means $\partial Y(p, q) = \partial H^\top(p, q) Y_0 H(p) + H^\top(p) Y_0 \partial H(p, q)$. As with $G(p)$, the parameter dependency described by $H(p)$ is a rational function such that the quadratic structure is maintained. Then the parameter dependency is factorised from (47b) to create an equivalent quadratic formulation where all parameter dependency is in the outer factors

$$Q_y^\top(p, q) Y_{0,mat} Q_y(p, q) < 0$$

where

$$Y_{0,mat} = \left[\begin{array}{cccccccc} 0 & Y_0 & & & & & & \\ Y_0 & 0 & & & & & & \\ & & -\gamma I & & & & & \\ & & & -\gamma I & & & & \\ & & & & 0 & I & & \\ & & & & I & 0 & & \\ & & & & & & -\gamma I & I \\ & & & & & & I & 0 \end{array}\right]$$

and

$$Q_y(p, q) = \left[\begin{array}{ccc} H\hat{A}^\top - \partial H & H\bar{C}_1^\top & 0 \\ H & 0 & 0 \\ \bar{B}_{12}^\top & 0 & 0 \\ 0 & I & 0 \\ 0 & 0 & \bar{B}_{11} \\ I & 0 & 0 \\ 0 & 0 & I \\ 0 & \bar{D}_1^\top & 0 \end{array}\right]. \tag{48}$$

The outer factor $Q_y(p, q)$ is cast into an upper LFT with a partitioned matrix $Q_{y,0}$ (see (3)). Then the full block S-Procedure with a multiplier Π_{Q_y}, as defined in Section II-A, is applied to condition (48). The following corollary states the resulting set of computationally solvable existence conditions for state-feedback control of an LPV plant.

Corollary 2. Let $\mathcal{P}$ be a given compact set and P_{SF} an LPV system as in (46) with measurable states x. There exists a stabilising state-feedback control law $F : u = F(\rho) x$ such that $\|F_l(P_{\text{SF}}, F(\rho))\| \leq \gamma$, where γ is a constant $\gamma > \bar{\sigma}(\bar{D}_1)$,

if there exists a continuously differentiable, symmetric matrix function $Y : \mathcal{P} \to \mathbb{R}^{n_x \times n_x}$ and a full block multiplier $\Pi_{Q_z} \in \mathbb{S}^{(n_1+m_1)\times(n_1+m_1)}$ with structure defined in Section II-A such that $\forall p \in \mathcal{P}$

$$Y_0 > 0 \tag{49a}$$

$$H^\top(0) Y_0 H(0) > 0 \tag{49b}$$

$$\left[\begin{array}{c|c} * & \end{array}\right]^\top \left[\begin{array}{c|c} \Pi_{Q_y} & \\ \hline & Y_{0,mat} \end{array}\right] \left[\begin{array}{cc} Q_{y,11} & Q_{y,12} \\ I & 0 \\ \hline Q_{y,21} & Q_{y,22} \end{array}\right] < 0, \tag{49c}$$

where $Y_{0,mat}$ and $Q_y(p)$ are defined in (48), $H(p)$ is a rational function, and $Q_{y,0}$ is the partitioned matrix of the upper LFT form (3) of $Q_y(p)$.

Much like for the filter synthesis, the constraint on the parameter dependency is satisfied as a result of the imposed structure on the full block multiplier Π_{Q_y}. Thus, the state-feedback synthesis is computationally solvable at the cost of some conservatism. In order to calculate the optimal controller gain, Corollary 2 is solved as an optimisation problem to minimise the performance metric γ that bounds the induced $\mathcal{L}_2$-norm of the weighted closed-loop system. Then the resulting un-scaled controller gain is calculated as $F(p) = -D_2^{-1}(\rho)(\gamma \bar{B}_{12}^\top(p) Y(p)^{-1} + \bar{C}_2(\rho))$.

IV. Application Example: Spacecraft Attitude Control

The derived structured control scheme and synthesis was applied to the attitude control of a small satellite benchmark. The computational effort and performance metrics of the structured synthesis were measured and compared to an output-feedback synthesis to verify that the proposed approach is far more efficient. Additionally, the different multiplier types, described in Section II-A, were compared in terms of conservatism and computational efficiency.

The satellite in question weighs 95 kg, and has a flexible solar array. The solar array is intentionally oversized in order to accentuate the effects of its flexible modes on the spacecraft dynamics. The lowest undamped frequency of its flexible modes is 5.6 rad/s. Additionally, the spacecraft is modelled with a draining fuel tank (no sloshing dynamics) positioned at the centre of mass of the central body. Hence, the mass properties of the spacecraft are time-varying. The spacecraft is in a sun-synchronous, 400 km altitude orbit. At this altitude, the considered disturbances (such as solar radiation pressure torque, aerodynamic torque, gravity gradient torque and magnetic torque) reach magnitudes of 1×10^{-3} Nm (see, e.g., [32]).

The spacecraft P is modelled with a cuboid, rigid central body $P_{\mathcal{B}}$ and a flexible solar array $P_{\mathcal{A}}$ modelled as a cantilever beam attached by a joint at point P as pictured in Figure 4. The position of the solar array's centre of mass is denoted A. The following spacecraft model was generated using the Satellite Dynamics Toolbox [33]; see the documentation for extensive explanation.

TABLE I
Parameters and notation used in (50) and Figure 4.

Parameters	Description
F_{ext}	Force vector applied to central body
$T_{ext,\mathrm{B}}$	Torque vector applied to central body at B
$F_{\mathcal{B}/\mathcal{A}}$	Force vector applied by $\mathcal{B}$ on $\mathcal{A}$
$T_{\mathcal{B}/\mathcal{A},\mathrm{P}}$	Torque vector applied by $\mathcal{B}$ on $\mathcal{A}$ at point P
$\ddot{r}$	Linear acceleration
$\ddot{\theta}$	Rotational acceleration
m	Mass
J	Inertia
τ_{AP}	Kinematic model between points A and P
Notation	**Denoting**
$\mathcal{B}$	Central body
B	Center of mass of central body
P	Position of joint
$\mathcal{A}$	Solar array
A	Center of mass of solar array

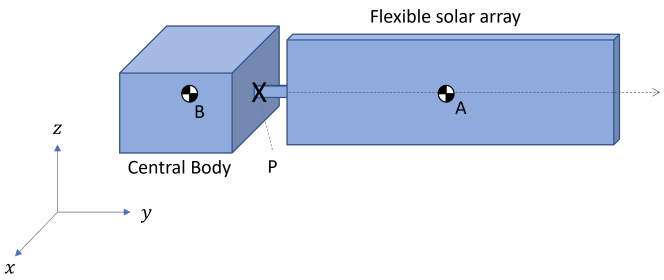

Fig. 4. Visual of spacecraft model

$$P_{\mathcal{B}} : \left[\begin{array}{c} F_{ext} \\ T_{ext,\mathrm{B}} \end{array}\right] = \left[\begin{array}{cc} m_{\mathcal{B}}(m_f) I & 0 \\ 0 & J_{\mathcal{B}}(m_f) \end{array}\right] \left[\begin{array}{c} \ddot{r}_{\mathrm{B}} \\ \ddot{\theta} \end{array}\right] + \left[\begin{array}{c} 0 \\ \dot{\theta} \times J_{\mathcal{B}} \dot{\theta} \end{array}\right]$$

$$P_{\mathcal{A}} : \left[\begin{array}{c} F_{\mathcal{B}/\mathcal{A}} \\ T_{\mathcal{B}/\mathcal{A},\mathrm{P}} \end{array}\right] = \tau_{\mathrm{AP}}^\top \left[\begin{array}{cc} m_{\mathcal{A}} I & 0 \\ 0 & J_{\mathcal{A}} \end{array}\right] \tau_{\mathrm{AP}} \left[\begin{array}{c} \ddot{r}_{\mathrm{P}} \\ \ddot{\theta} + \ddot{\theta}_{\mathcal{A}} \end{array}\right] + L_{\mathrm{P}}^\top \ddot{\eta}$$

$$-L_{\mathrm{P}} \left[\begin{array}{c} \ddot{r}_{\mathrm{P}} \\ \ddot{\theta} + \ddot{\theta}_{\mathcal{A}} \end{array}\right] = \ddot{\eta} + diag\{2\zeta_i \omega_i\}_{i=1}^3 \dot{\eta} + diag\{\omega_i^2\}_{i=1}^3 \eta \tag{50}$$

See Table I for details of the notation. The central body experiences external forces F_{ext} and torques T_{ext} about the centre of mass. The dynamic coupling between the two bodies is transmitted via the joint at point P. The flexible modes of the solar array are described by their modal contributions L_{P}. Each second-order mode (denoted by subscript i) has damping ζ_i and natural frequency ω_i.

The central body mass $m_{\mathcal{B}}$ is a function of the fuel mass m_f, which is calculated from the commanded torque u and specific impulse $\mathrm{I_{sp}}$ using the thrust equation. The central body inertia about the centre of mass $J_{\mathcal{B}}$ also changes with fuel mass. To exaggerate the effects of the changing mass properties, it is assumed that 25% of the spacecraft's total mass is fuel. For this application, only rotational dynamics are considered for attitude control, so the translational motion r of the central body is disregarded. For the control problem,

TABLE II
TUNING PARAMETERS FOR THE SYNTHESIS OF ALL CONTROLLERS. $\text{diag}([a_1,\ a_2,\ a_3])$ DENOTES A DIAGONAL MATRIX WITH ELEMENTS a_1, a_2, a_3 ON THE DIAGONAL.

W_u	$=$	$\frac{0.667s+0.0115}{s+2.015\times10^{-5}} \cdot I_{3\times3}$
W_e	$=$	$\frac{100s+50}{s+50} \cdot I_{3\times3}$
V_u	$=$	$\text{diag}([2,\ 1.5,\ 2])$
V_e	$=$	$0.0014 \cdot I_{3\times3}$
V_d	$=$	$0.01 \cdot \text{diag}([1,\ 0.2,\ 1])$

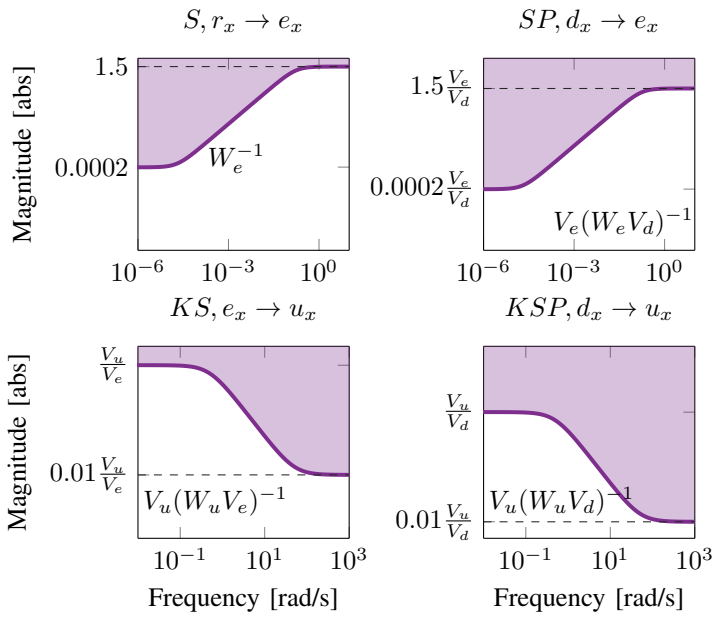

Fig. 5. Visualisation of imposed performance on transfer functions (four blocks) about the x-Axis. Similar plots exist for transfer functions between all axes (including cross-coupling).

the system output is the attitude θ which must track a target attitude relative to an inertial frame. The external disturbances are modelled as a summative input disturbance on the commanded torque $T_{ext} = d + u$. Hence, the linear plant takes the general LPV plant structure in (17).

The application case considered in this paper is a slew manoeuvre using thrusters. The controller is synthesised with m_f as the scheduling parameter ρ. Consider three thrusters provide torque about each axis of the spacecraft. They are each positioned with a lever arm of 10 cm from the centre of mass of the central body. The maximum force produced by each thruster is assumed to be 20 N with an I_{sp} of 100 s as this is reasonable for a small satellite [34]. This results in a maximum torque about each axis of 2 Nm and maximum mass loss rate of 0.02 kg/s, which is used as the rate-bound in the synthesis. The guidance profile, which the spacecraft must follow for the slew, is generated as a rectangular acceleration signal, then integrated twice to provide a reference attitude signal.

A. Controller Design and Synthesis

All controllers were synthesised using the same design and tuning weights such that meaningful comparisons and conclusions could be drawn. For each multiplier, the structured controller K_S was synthesised once with a parameter-varying slack variable $U(\rho)$, and again with static slack variable U for additional comparison. In addition, an output-feedback controller K_{OF} was synthesised for each multiplier in order to compare the synthesis efficiency and controller performance. The output-feedback controllers were also synthesised in LFT formulation by applying the transformation process described in this paper to the output-feedback problem (see the thesis of Wu [7]). All syntheses were 10% sub-optimal to improve numerical behaviour and used an identical weighting scheme (see (18) and Figure 1). In the presented application, the weighting scheme is LTI.

All tuning design variables are listed in Table II. The command weight W_u enforces that the controller does not have a high magnitude in the region of the flexible modes for all three axes. W_e was selected to enforce good tracking by shaping the sensitivity function, therefore the desired crossover frequency was iteratively increased during the tuning process. W_e also enforces the sensitivity peak to remain below 3.5 dB and the steady-state tracking error with respect to the reference command to be $< 1.8 \times 10^{-4}$. The aggressiveness of the actuators is defined by V_u/V_e. In this design, for example, an error signal e_x of 0.01 rad, can result in a torque command of up to 1.8 Nm, which aligns with the implementation of a thruster slew. Given that the solar array is aligned to the body-frame y-axis, less torque is required about this axis to accelerate so less authority was given about this axis. Then, V_d is approximately 10 times the magnitude of environmental torque disturbances at 400 km altitude. With respect to the disturbance rejection, this choice of V_d imposes that the disturbance signal cannot be amplified more than $1.5 \cdot V_e/V_d = 0.21$ in the x and z axes (which were given higher torque authority), and 1 in the y-axis (accounting for 3.5 dB maximum magnitude in S, see Figure 5 for clarification). This preference for better disturbance rejection about x and z also reflects the lower level of torque disturbance that would occur about the y-axis due to the shape of the satellite. Note that for low frequency, amplification of disturbance is significantly lower due to the shape of W_e. Similarly, V_u/V_d describes how aggressively the controller can respond to the disturbance.

The first stage of the controller synthesis for K_S with each multiplier was to calculate the filter gain $L(\rho) = (G^\top(\rho)Z_0G(\rho))^{-1}C_{sc}^\top V_e^{-1}$ in the filter synthesis step, see Section III-B. This was done by applying the optimisation

from Corollary 1 to the rigid model of the spacecraft's response to external disturbances $P_{sc} = V_e^{-1}P(\rho)V_d$. The parameter variation is quadratic $G(p) = [I,\ pI]^\top$. After the filter gain was calculated, the contractive left-coprime factorisation of the scaled plant $[M_{sc},\ N_{sc}]$ was reconstructed. Using M^{-1} and the designed weighting scheme, the state-feedback problem was defined (see Section III). The state-feedback synthesis step solved the optimisation in Corollary 2 for the weighted system, constructed as in (34). The resulting controller gain $F(\rho)$, filter gain $L(\rho)$ and system state and input matrices form the structured controller pictured in Figure 3. For each K_{OF}, there was only one synthesis step and the resulting controller had the same number of states but no discernible structure.

For synthesis, the varying parameter was normalised so that Theorem 2 is applicable with the full block multipliers described in Section II-A.

B. Results to Confirm Theory

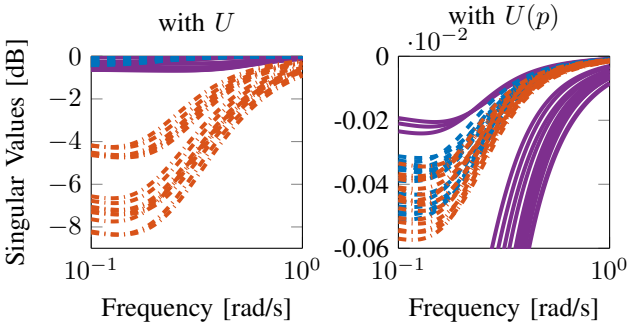

Fig. 6. Singular values of contractive left-coprime factorisation $[M_{sc},\ N_{sc}]$ for synthesis with block-diagonal (-·-·-), full-block (- - -) and parameter-dependent (——) multipliers.

The results for the first stage of the structured synthesis are displayed in Figure 6. Here, the singular values of the left-coprime factorisation are plotted for the respective multipliers, and for static or parameter-dependent slack variables (U and $U(p)$, respectively). For the static slack variable case, there is a clear reduction in conservatism for the full-block and parameter-dependent multipliers when compared to the block-diagonal case. However, the same correlation is not so clear when using $U(p)$. It is important to consider the complexity of the optimisation introduced by each multiplier as this is also an influencing factor in the optimisation. For each application of the full block S-procedure (as in Section II-A), the block-diagonal multipliers add additional LMI constraints with dimension $2n_\Delta + n_{in}$ where Δ is the size of the Δ-block and n_{in} the input dimension of the outer factor $G(p)$. This scales linearly with the size of the system and complexity of parameter variation or number of parameters. On the other hand, the additional LMI constraints when using the full-block multiplier has dimension $2n_\Delta + n_{in} + 2^{n_\delta} n_\Delta$ as a result of evaluating (10) at the vertices of Δ. This already exhibits poorer scaling with more scheduling parameters or increasing complexity of parameter-dependency. Furthermore, with the parameter-dependent multiplier, the larger LMI in

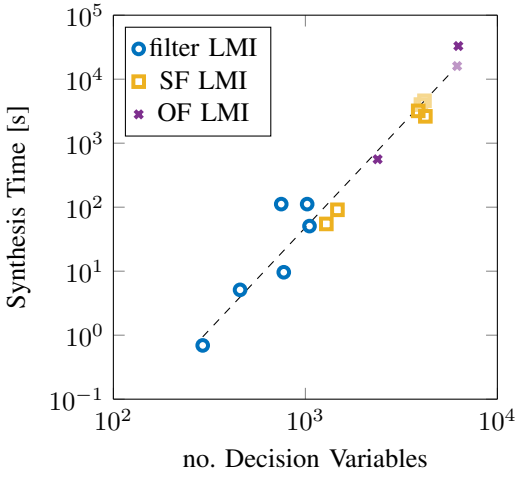

Fig. 7. Correlation between size of SDP and synthesis time. Paler coloured points on the correlation line correspond to failed syntheses who's no. of decision variables is known but synthesis time is not computed.

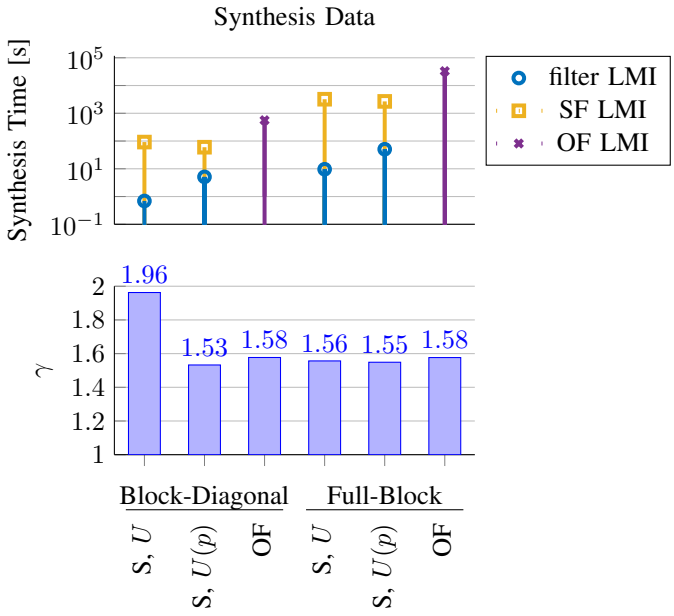

Fig. 8. Stacked, logarithmic plot of computation time (above) for the filter and state-feedback (SF) LMIs, and corresponding performance value (below) for each multiplier type.

the full block S-procedure (9) is evaluated at the vertices of Δ, so the resulting additional LMI dimensions for one application of the procedure is $2^{n_\delta}(n\Delta + n_{in})$. For simple problems, this may lead to a smaller optimisation than the full-block multiplier in terms of size, but the complexity of the additional LMIs is higher. Also, with more scheduling parameters it scales even worse. In this application, when the full block S-procedure is applied to, for example, 37b, $n_\delta = 2$ (p and q) and $n_{in} = 9$. With a static slack variable $n_\Delta = 6$ and the additional LMI dimensions are 21, 45 and 60 for block-diagonal, full-block and parameter-dependent multipliers, respectively. Comparatively, with a parameter-dependent slack variable $n_\Delta = 12$ and the dimensions grow to 33, 81 and 72. As a result, the optimisations for full-

block and parameter-dependent multipliers with $U(p)$ were unable to fully converge to an optimal solution and instead terminated the algorithm when the objective was decreased no more than 1% in the last 10 iterations. The objective values were therefore slightly higher, at 3.94×10^{-6} and 1.88×10^{-6} respectively, compared to the block-diagonal case 1.73×10^{-6}.

As a result of the dimension and complexity of the additional LMIs in the parameter-dependent multiplier cases, the optimisation was unable to find a solution to the state-feedback problems. Therefore, only 6 controllers have been synthesised. Three for each remaining multiplier corresponding to structured controllers with static and parameter-dependent slack variables (K_S, U and K_S, $U(p)$) and an output-feedback controller (K_{OF}).

The synthesis performance and efficiency are summarised in Figure 8. The controllers' performance is measured by the γ-value of the optimisation. A lower value corresponds to a controller that is better at meeting the requirements imposed by the weighting scheme across the parameter domain. In terms of computational effort, the syntheses for K_S in each case takes considerably less time to compute than the K_{OF} syntheses. With the block-diagonal multiplier, K_S synthesises approximately 6 times faster than K_{OF}, this improvement increasingly scales as the complexity of the problem grows. With the full-block multiplier K_S is synthesised more than 10 times faster than the corresponding K_{OF} which took approximately 9 hours to compute. Figure 7 confirms that the synthesis time correlates with the number of decision variables in the SDP. So, as control design problems get more complex, it is increasingly important to find ways to reduce the size of the SDPs. All optimisations in the presented work used the same methods and solver (`Lmilab`) with the same solver settings so that the comparison is as meaningful as possible. The relative accuracy required of the solution to the objective function in the optimisation is 0.01. This applies to the output-feedback problem, state-feedback problem and the coprime factorisation. Of course, with different solvers, computational time and accuracy will change so it is perhaps more valuable to look at the size of the SDPs (see Figure 7) and LMI dimensions as an indication of how complex (and therefore slow) computation of the optimal solution will be.

It is also demonstrated by the results that a varying slack variable $U(p)$ can lead to a better coprime factorisation (see Figure 6) with less divergence from I, although this may not always be the case. As a result, this can reduce conservatism in the solution, which is evident in the performance values γ displayed in Figure 8, especially for the block-diagonal case. Generally, a larger γ-value corresponds to more conservatism, which in turn correlates with poorer coprime factorisation in the filter synthesis step. It is further demonstrated that the low level of conservatism introduced by $[M,\ N]$, results in the overall performance of the structured design being very close to the performance of the output-feedback design. An indication of how the controllers each perform with respect to the imposed requirements is visually represented in Figure 9 by Bode diagrams of the transfer functions that are shaped during the syntheses. Only two of the four-block transfer functions that were the main drivers in the design are plotted for brevity. Additionally, the K_S controllers with parameter varying slack variable $U(\rho)$ have been omitted from the plots for clarity, as they were very similar to their corresponding static slack variable controllers. These plots show an array of each parameter-dependent closed-loop transfer function, where the array domain for each is linearly distributed across $-1 \leq \rho \leq 1$. Figure 9 further confirms that both synthesis methods lead to very similar controllers and demonstrates that the structured approach, performing the optimisation with the two-block problem, still shapes all four blocks in the original design. Note that the magnitude of KS peaks below the imposed magnitude of the design, so the actuator response is less aggressive in the final simulations than anticipated in the design.

TABLE III
ROBUSTNESS PERFORMANCE FOR ALL CONTROLLERS.

Multiplier	Controller	Worst loop-at-a-time margin across ρ		
		Gain [dB]	Phase [°]	Delay [s]
block-diagonal	K_S, U	12.58	43.04	1.36
	K_S, $U(p)$	12.28	43.35	1.96
	K_{OF}	7.43	35.67	0.77
full-block	K_S, U	12.31	43.63	1.94
	K_S, $U(p)$	12.31	43.55	1.97
	K_{OF}	7.46	35.67	0.77

The K_S loops demonstrate slightly lower crossover frequency in the sensitivity function, and marginally increased magnitude in SP compared to the K_{OF} loops. Ultimately, this plot demonstrates that all the controllers exhibit very similar loop-shapes. This is unsurprising, given the similar γ-values. This further demonstrates that it is advantageous to use the structured synthesis method to save on computational time without sacrificing performance. Moreover, the full-block multiplier does not show significant improvement over the block-diagonal multiplier. So, whereas it does objectively reduce the conservatism, in many practical applications, the simplest and most efficient multiplier choice is sufficient. The worst-case loop-at-a-time margins are also provided in table III to further confirm the similarity of the controllers. It is also seen that the OF controllers sacrifice some robustness margins in order to push the performance further. These conclusions are further reiterated in the time-domain simulations in Figure 10.

In the simulations, K_{OF} shows a slight improvement compared to K_S with a reduced attitude error $|e|$. This results from the higher crossover frequency in the sensitivity function which enables improved tracking. Additionally, K_{OF} with the full-block multiplier performs slightly better, correlating with the reduced conservatism. All structured controllers K_S perform almost identically, irrespective of the choice of multiplier. Hence, they have been plotted as a single line for clarity. The largest variation in error $|e|$ between all structured controllers is 0.01 rad which occurs at approximately 34 s where the largest overshoot is in each slew. The time-domain simulations further establish the consistency in performance across the domain of the scheduling parameter. The performance is the same when completing a slew at the beginning of life (BoL), where fuel mass is initialised at the maximum value, and

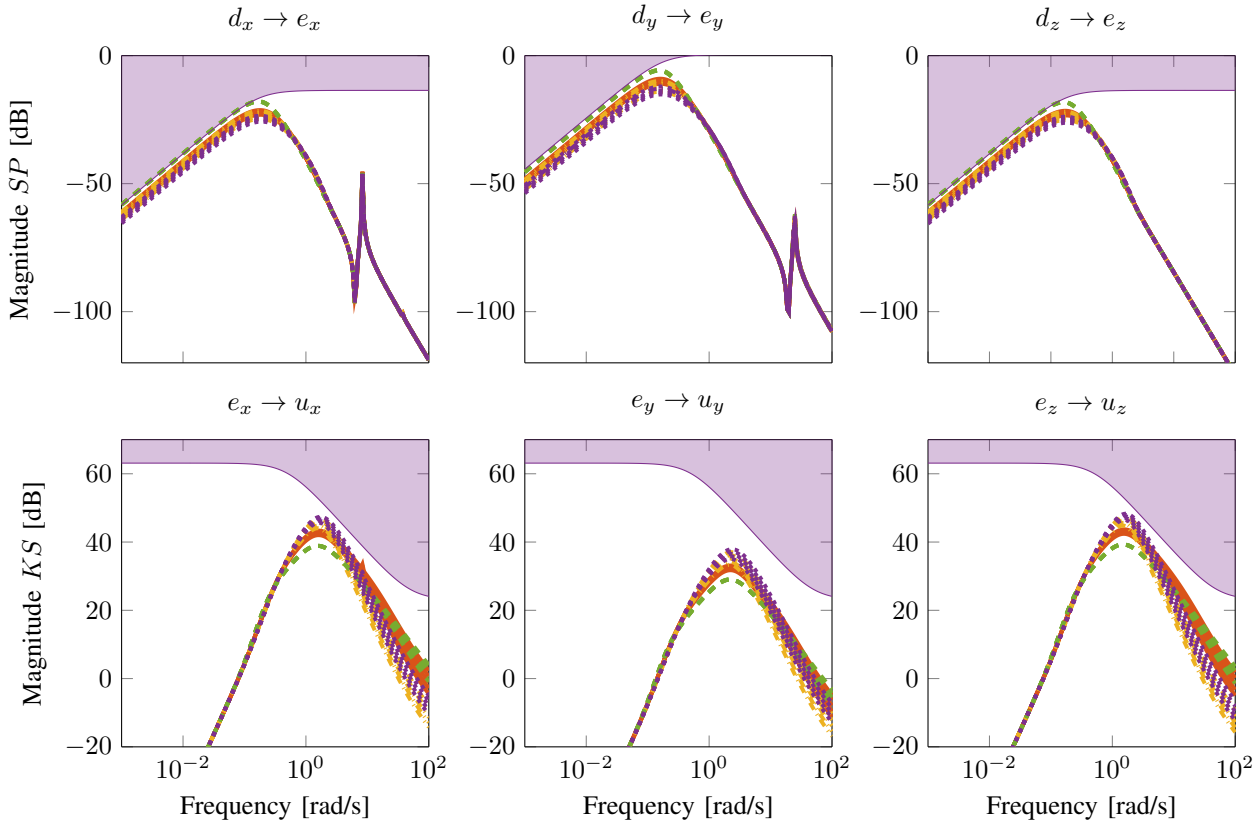

Fig. 9. Resulting loop-shapes of K_S controller with U, block-diagonal and full-block multipliers (——,– – –), K_{OF} controller with block-diagonal and full-block multiplier (–·–,·····) with respect to design constraints.

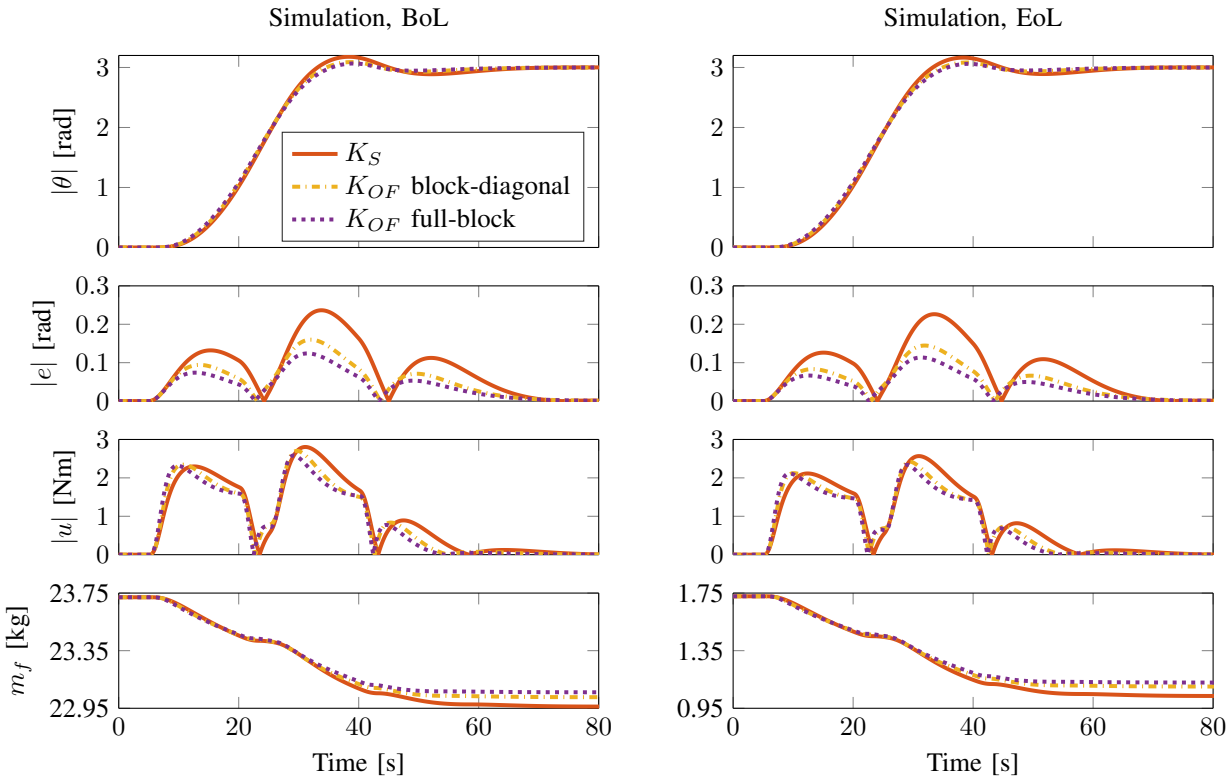

Fig. 10. Tracking performance for controllers at the beginning of life (BoL) and end of life (EoL). All structured controllers K_S are represented with one line.

end of life (EoL), where the fuel mass is almost empty. As expected, the controllers in the EoL slew scenario command smaller values $|u|$ and burn slightly less fuel as the overall mass of the spacecraft is less, so requires less torque from the thrusters.

Note that the results presented in this section correspond to a synthesis computed on a standard desktop PC with a modern i7, 8-core processor at 3.80 GHz and 32 GB of RAM.

V. Conclusion

A structured controller synthesis in LFT formulation was derived and presented as a novel approach to the control of LPV systems. In general, LFT formulation is preferable to grid-based LPV methods when it comes to scheduled controllers as it offers a closed solution without approximation steps in the derivation. Although, the LFT formulation does require that the parameter variation can be reasonably approximated by rational polynomials. The presented method also results in a highly structured controller which is beneficial for implementation.

The presented design process used a recently proposed weighting scheme to impose physically quantifiable and unambiguous requirements on the controller. The same weighting scheme was also applied to an output-feedback controller synthesis such that a reasonable baseline comparison could be drawn. The chosen use-case was a small spacecraft performing slew manoeuvres with fuel mass as a scheduling parameter. The presented two-step synthesis was considerably less computationally expensive than the output-feedback synthesis while not compromising on performance. It was also demonstrated that the computational benefit was further increased when scaling up to more complicated design problem with less conservative multipliers. However, it has been shown that the simplest multiplier choice may be sufficient in terms of achieved performance.

References

[1] H. Pfifer, C. P. Moreno, J. Theis, A. Kotikapuldi, A. Gupta, B. Takarics, and P. Seiler, "Linear Parameter Varying Techniques Applied to Aeroservoelastic Aircraft: In Memory of Gary Balas," *IFAC-PapersOnLine*, vol. 48, no. 26, pp. 103–108, 2015. [Online]. Available: https://linkinghub.elsevier.com/retrieve/pii/S2405896315023794

[2] E. Burgin, F. Biertümpfel, and H. Pfifer, "Linear parameter varying controller design for satellite attitude control," in *22nd IFAC World Congress*, 2023, pp. 3455–3460.

[3] H. Seif-El-Islam and L. Abdou, "Robust LPV control for attitude stabilization of a quadrotor helicopter under input saturations," *Advances in Technology Innovation*, vol. 5, no. 2, p. 98, 2020.

[4] S. Liu, J. F. Whidborne, and S. Chumalee, "Disturbance observer enhanced neural network LPV control for a blended-wing-body large aircraft," *IEEE Transactions on Aerospace and Electronic Systems*, vol. 57, no. 5, pp. 2689–2703, 2021.

[5] H. Atoui, O. Sename, V. Milanés, and J. J. Martinez, "LPV-based autonomous vehicle lateral controllers: A comparative analysis," *IEEE Transactions on Intelligent Transportation Systems*, vol. 23, no. 8, pp. 13 570–13 581, 2021.

[6] H. Atoui, O. Sename, V. Milanes, and J.-J. Martinez-Molina, "Toward switching/interpolating LPV control: A review," *Annual Reviews in Control*, vol. 54, pp. 49–67, 2022.

[7] F. Wu, X. H. Yang, A. Packard, and G. Becker, "Induced L2-norm control for LPV systems with bounded parameter variation rates," *Int J Robust and Nonlinear Control*, vol. 6, no. 9-10, pp. 983–998, 1996.

[8] A. Packard, "Gain scheduling via linear fractional transformations," *Systems & Control Letters*, vol. 22, no. 2, pp. 79–92, 1994. [Online]. Available: https://linkinghub.elsevier.com/retrieve/pii/0167691194901023

[9] C. Scherer, "LPV Control and Full Block Multipliers," *Automatica*, vol. 37, no. 3, pp. 361–375, 2001.

[10] C. Roos, "Generation of flexible aircraft LFT models for robustness analysis," *IFAC Proceedings Volumes*, vol. 42, no. 6, pp. 349–354, 2009.

[11] S. Winkler, M. Martin, R. Geshnizjani, H. Pfifer, F. Biertümpfel, L. Hafemeister, and E. Pelletier, "De-risk new AOCS/GNC V&V technologies for industrial efficiency," in *43rd Annual AAS Guidance and Control Conference*, vol. 30, no. 563, 2020, pp. 1461–1472.

[12] F. Saupe and H. Pfifer, "An Observer Based State Feedback LFT LPV Controller for an Industrial Manipulator," *IFAC Proceedings Volumes*, vol. 45, no. 13, pp. 337–342, 2012. [Online]. Available: https://linkinghub.elsevier.com/retrieve/pii/S1474667015377119

[13] J. Theis, H. Pfifer, and P. Seiler, "Robust Modal Damping Control for Active Flutter Suppression," *Journal of Guidance, Control, and Dynamics*, vol. 43, no. 6, pp. 1056–1068, 2020. [Online]. Available: https://arc.aiaa.org/doi/10.2514/1.G004846

[14] J. Theis and H. Pfifer, "Observer-Based Synthesis of Linear Parameter-Varying Mixed Sensitivity Controllers," *Int J Robust Nonlinear Control*, vol. 30, pp. 5021–5039, 2020.

[15] C. W. Scherer, "A full block S-procedure with applications," in *Proceedings of the 36th IEEE Conference on Decision and Control*, vol. 3. IEEE, 1997, pp. 2602–2607.

[16] E. Prempain, "On Coprime Factors for Parameter-Dependent Systems," in *45th Conference on Decision and Control*. IEEE, 2006, pp. 5796–5800.

[17] E. Prempain and I. Postlethwaite, "L2 and H2 performance analysis and gain-scheduling synthesis for parameter-dependent systems," *Automatica*, vol. 44, no. 8, pp. 2081–2089, 2008.

[18] D. C. McFarlane and K. Glover, "A Loop-Shaping Design Procedure Using H-infinity Synthesis," *IEEE Transactions on Automatic Control*, vol. 37, no. 6, pp. 759–769, 1992.

[19] R. L. Pereira and M. S. de Oliveira, "Mixed-sensitivity L2 controller synthesis for discrete-time LPV/LFR systems," *Journal of the Franklin Institute*, vol. 359, no. 2, pp. 1062–1085, 2022. [Online]. Available: https://linkinghub.elsevier.com/retrieve/pii/S0016003221006864

[20] F. Wu, *Control of Linear Parameter Varying Systems*. University of California, Berkeley, 1995.

[21] F. Wu and K. Dong, "Gain-Scheduling Control of LFT Systems Using Parameter-Dependent Lyapunov Functions," *Automatica*, vol. 42, no. 1, pp. 39–50, 2006.

[22] H. Pfifer, *LPV/LFT Modeling and Its Application in Aerospace*. Technische Universität München, 2013.

[23] M. Vidyasagar, *Control System Synthesis: A Factorization Approach*, 1st ed. The MIT Press, 1985.

[24] R. S. Sanchez-Peña and M. Sznaier, *Robust Systems Theory and Applications*, 1st ed. John Wiley & Sons, 1998.

[25] G. D. Wood, *Control of Parameter-Dependent Mechanical Systems*. University Cambridge, 1995.

[26] D. C. McFarlane and K. Glover, *Robust controller design using normalized coprime factor plant descriptions*. Springer, 1990.

[27] M. G. Safonov, D. Limebeer, and R. Chiang, "Simplifying the H infinity theory via loop-shifting, matrix-pencil and descriptor concepts," *International Journal of Control*, vol. 50, no. 6, pp. 2467–2488, 1989.

[28] J. Theis, D. Ossmann, F. Thielecke, and H. Pfifer, "Robust autopilot design for landing a large civil aircraft in crosswind," *Control Engineering Practice*, vol. 76, pp. 54–64, 2018. [Online]. Available: https://linkinghub.elsevier.com/retrieve/pii/S0967066118300911

[29] J. Theis, N. Sedlmair, F. Thielecke, and H. Pfifer, "Observer-based LPV Control with Anti-Windup Compensation: A Flight Control Example," *IFAC-PapersOnLine*, vol. 53, no. 2, pp. 7325–7330, 2020.

[30] S. Skogestad and I. Postlethwaite, *Multivariable Feedback Control: Analysis and Design*. john Wiley & sons, 2005.

[31] G. Meinsma, "Unstable and nonproper weights in H infinity control," *Automatica*, vol. 31, no. 11, pp. 1655–1658, 1995.

[32] P. C. Hughes, *Spacecraft attitude dynamics*. Courier Corporation, 2012.

[33] D. Alazard and F. Sanfedino, "Satellite dynamics toolbox for preliminary design phase," in *43rd Annual AAS Guidance and Control Conference*, vol. 30, no. 563, 2020, pp. 1461–1472.

[34] V. Zakirov, M. Sweeting, P. Erichsen, and T. Lawrence, "Specifics of small satellite propulsion: Part 1," in *15th AIAA/USU Conference on Small Satellites*, 2001.

Emily Burgin is currently a doctoral candidate at the Technische Universität Dresden, Germany, co-sponsored by the European Space Agency. The focus of her research is the theory and application of linear parameter-varying techniques to aerospace systems within the robust control framework. She received her Master's degree in Aerospace Engineering from The University of Nottingham, England, in 2021. Since then, she worked as a guidance, navigation and control engineer in the space sector (Deimos Space UK) before pursuing a PhD.

Harald Pfifer holds the Chair in Flight Mechanics and Control at Technische Universität Dresden, Germany. He received his Ph.D. from Technical University Munich, Germany, in 2013. Before joining Technische Universität Dresden in 2021, he was an assistant professor at University of Nottingham, and a post-doctoral associate at University of Minnesota. His main research interests include aeroservoelastic control, uncertain dynamical systems, and robust and linear parameter-varying control.